Journal of Medicinal Chemistry Letter

J. Med. Chem. **2009,** *52,* 5009–5012 **5009**
DOI: 10.1021/jm900725r

Discovery of a Highly Potent, Selective, and Bioavailable Soluble Epoxide Hydrolase Inhibitor with Excellent Ex Vivo Target Engagement

Hong C. Shen,* Fa-Xiang Ding, Siyi Wang, Qiaolin Deng, Xiaoping Zhang, Yuli Chen, Gaochao Zhou, Suoyu Xu, Hsuan-shen Chen, Xinchun Tong, Vincent Tong, Kaushik Mitra, Sanjeev Kumar, Christine Tsai, Andra S. Stevenson, Lee-Yuh Pai, Magdalena Alonso-Galicia, Xiaoli Chen, Stephen M. Soisson, Sophie Roy, Bei Zhang, James R. Tata, Joel P. Berger, and Steven L. Colletti

Merck Research Laboratories, Merck & Co., Inc., Rahway, New Jersey 07065-0900

Received March 5, 2009

Abstract: 4-Substituted piperidine-derived trisubstituted ureas are reported as highly potent and selective inhibitors for sEH. The SAR outlines approaches to improve activity against sEH and reduce ion channel and CYP liability. With minimal off-target activity and a good PK profile, the benchmark **2d** exhibited remarkable in vitro and ex vivo target engagement. The eutomer *ent*A-**2d** also elicited vasodilation effect in rat mesenteric artery.

Epoxide hydrolases are a group of ubiquitous enzymes detected in species ranging from plants to mammals.[1] These enzymes catalyze the addition of water to an epoxide, resulting in the formation of a vicinal diol. Several types of epoxide hydrolases have been identified including sEH,[a] mEH, cholesterol epoxide hydrolase, LTA_4 hydrolase, and hepoxilin hydrolase.[2] These epoxide hydrolases differ in their substrate specificity. For example, sEH is selective for aliphatic epoxides such as fatty acid epoxides while mEH is more selective for cyclic and arene epoxides. The major known physiological substrates of sEH are the four regioisomeric epoxides of arachidonic acid, namely, 5,6-, 8,9-, 11,12-, and 14,15-epoxyeicosatrienoic acids (also known as EETs) and epoxides of linoleic acid.[1] The corresponding diol products of sEH-mediated hydrolysis of EETs are referred to as DHETs.

EETs elicit a wide range of biological effects.[3] They are known to vasodilate coronary arterioles and renal microvessels via the activation of BK_{Ca} ion channels.[4] Notably, 11,12-EET has been identified as EDHF, a long-sought endogenous metabolite with robust vascular smooth muscle relaxing activity.[5] EETs, and especially 11,12-EET, have also exhibited antiinflammatory activities, apparently by decreasing the expression of cytokine induced endothelial cell adhesion molecules, such as VCAM-1.[6] In addition, EETs prevented leukocyte adhesion to the vascular wall, presumably by inhibiting NFκB and IKB kinases.[7] Hence, it is conceivable that EET elevation resulting from sEH inhibition could inhibit the NFκB pathway and thus ameliorate vascular inflammation. These properties suggest a potential application of sEH inhibitors to the mitigation of endothelial dysfunction.

Recent studies in preclinincal species indicated that sEH inhibition could be useful for the treatment of hypertension and disease-modifying end organ protection. For example, it has been reported that sEH inhibitors could significantly reduce blood pressure in angiotensin II treated rats[8] and SHRs.[9] Additionally, treatment with an sEH inhibitor in angiotensin II infused hypertensive rats attenuated the afferent kidney arteriolar diameter and reduced urinary albumin secretion, a marker of compromised renal function. As such, an sEH inhibitor will soon be evaluated in a phase II clinical trial for metabolic syndrome indications.[10]

Despite some known sEH inhibitors,[11] there remained a significant challenge to develop sEH inhibitors with enhanced potency, improved solubility and PK, and high selectivity against other biological targets, particularly ion channels, CYP enzymes, and targets that could lead to undesirable pharmacological consequences. Herein, we report the identification of 4-substituted piperidine-derived trisubstituted ureas as potent and selective sEH inhibitors (Figure 1), which served as exploratory tools to examine sEH pharmacology. It is noted that disubsituted ureas are typically associated with poor PK and physical properties. The trisubstituted ureas, however, clearly demonstrated improved PK and superior physical properties.

All analogues were tested in human and rat sEH inhibition assays. Potent compounds were also subject to cell-based DHET production assay to examine their cellular sEH inhibitory activity. Because of the significant roles of mEH in xenobiotic detoxication and steroid metabolism, the inhibition of this enzyme posed a safety concern. Therefore, mEH became a major target for counterscreen, although few compounds were known to be inhibitors of both enzymes.[12] Additionally, CYP2C9, 2D6, and 3A4 were selected as routine counterscreening targets. Of particular importance within this cohort of enzymes is CYP2C9, as it is involved in producing EETs via the monooxygenase-mediated epoxidation of arachidonic acid.[3a] Therefore, elevation of EETs by sEH inhibition could be diminished by simultaneous CYP2C9 inhibition. Furthermore, cardiac potassium (IKr),[13] calcium (DLZ binding or $Ca_v1.2$ functional assays),[14] and sodium ($Na_v1.5$)[15] channels were scrutinized on the basis of their potential blood pressure and cardiac effects.

To the best of our knowledge, the previous reports on sEH inhibitors did not disclose whether they had ion channel or CYP inhibitory activities. This is a critical omission, since in order to evaluate the antihypertensive effects of sEH inhibitors, it is a prerequisite that they demonstrate strong sEH engagement, without off-target activity that could by itself impact blood pressure change. In addition, a telemetry

*To whom correspondence should be addressed. Phone: 732-594-1755. Fax: 732-594-9473. E-mail: hong_shen@merck.com.

[a] Abbreviations: sEH, soluble epoxide hydrolase; mEH, microsomal epoxide hydrolase; LTA_4, leukotriene A_4; EDHF, endothelial derived hyperpolarization factor; EET, epoxyeicosatrienoic acid; DHET, dihydroepoxyeicosatrienoic acid; SHR, spontaneously hypertensive rats; VCAM-1, vascular cell adhesion molecule 1; NFκB, nuclear factor κB; COX-2, cyclooxygenase-2; PGE_2, prostaglandin E_2; PGD_2, prostaglandin D_2; SHR, spontaneously hypertensive rats; PK, pharmacokinetics; CYP, cytochrome P450; DLZ, diltiazem; SAR, structure−activity relationship; SFC, supercritical fluid chromatography; 20-HETE, 20-hydroxyeicosatetraenoic acid.

Published on Web 07/31/2009

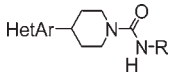

Figure 1. Scaffold of trisubstituted urea sEH inhibitors.

Table 1. In Vitro SAR on sEH and mEH Inhibition, DHET Production, CYP and Ion Channels[a]

Compds	IC_{50} (h, r) (nM)	DHET IC_{50}, (nM)[b]	mEH IC_{50} (μM)[c]	CYP2C9, 2D6, 3A4 IC_{50} (μM)	$Ca_v1.2$, IKr $Na_v1.5$, IC_{50} (μM)
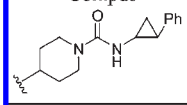					
 1a	430, 290	3619	14	>10, >10, >10	>30, >30, >10
 1b	120, 170	2208	>100	>10, >10, >10	11, >30, >10
 1c	8400, 20000	>20000	>100	>10, >10, >10	>30, >30, >10
 1d	1100, 180	1432	>100	>10, >10, >10	>30, >30, >10
 1e	480, 130	2439	>100	>10, >10, >10	>30, >30, >10
 1f	1100, 350	>20000	>100	>10, >10, >10	>30, >30, >10
 1g	235, 207	240	>100	>10, >10, >10	>30, 27, >10
 1h	54, 56	333	>100	>10, >10, >10	>30, >30, >10
 1i	28, 48	<1	>100	>10, >10, >10	>30, >30, >10
 1j	7.5, 16	8	67	<10, >10, >10	12, 8.2, ~10

[a] Activity was determined in triplicate with 20% deviation. [b] The conversion of 14,15-EET to 14,15-DHET was measured in HEK293 cells. [c] Human mEH was used.

Table 2. In Vitro SAR on sEH and mEH Inhibition, DHET Production, CYP and Ion Channels[a]

Compds	IC_{50} (h, r) (nM)	DHET IC_{50}, (nM)[b]	mEH IC_{50} (μM)[c]	CYP2C9, 2D6, 3A4 IC_{50} (μM)	DLZ, IKr $Na_v1.5$ IC_{50} (μM)
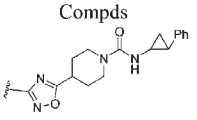					
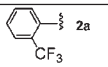 2a	9, 6	7	19	~10, >10, >10	2, 6, <10
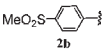 2b	4, 12	11	42	>10, >10, >10	>30, 9, >10
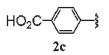 2c	5, 17	190	>100	>10, >10, >10	>30, >30, >10
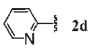 2d	9, 10	34	>100	>10, >10, >10	>30, >30, >10
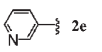 2e	7, 10	13	>100	>10, >10, <10	19, 2, >10
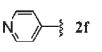 2f	14, 15	30	>100	>10, >10, >10	>30, 10, >10
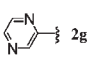 2g	13, 17	11	>100	>10, >10, >10	>30, 27, >10
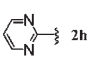 2h	33, 35	187	>100	<10, >10, >10	>30, >30, >10
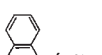 2i	10, 21	35	>100	<10, >10, >10	3, 7, <10
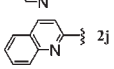 2j	7, 8	7	7	>10, >10, <10	6.8, 2.6, <10
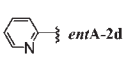 *ent*A-2d	14, 27	18	>100	>10, >10, >10	>30, >30, >10
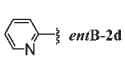 *ent*B-2d	62, 18	176	>100	>10, >10, >10	>30, >30, >10

[a] Activity was determined in triplicate with 20% deviation. [b] The conversion of 14,15-EET to 14,15-DHET was measured in HEK293 cells. [c] Human mEH was used.

method was employed for the SHR model, thus providing a reliable tool to monitor blood pressure.

First, the 4-position of piperidine was systematically studied with benzene and various six-membered heterocycles. These analogues generally gave poor enzyme inhibitory activity (data not shown). In contrast, use of five-membered polar heterocycles led to improved activity (Table 1). In particular, oxadiazole regioisomer **1i** offered the best enzymatic and cellular activity, indicating its good cell permeability. It is noted that most compounds with a 4-heteroaryl group in Table 1 provided very clean off-target profiles with regard to mEH (IC_{50} > 100 μM), ion channels (IC_{50} > 10 μM), and CYP enzyme (IC_{50} > 10 μM) inhibition.

The choice of heterocycle proved to be critical, as small changes in structure resulted in massive changes in sEH activity. Adopting the requisite oxadiazole shown in **1i** as the optimized fragment, additional aryl substitution of oxadiazole further diminished the sEH IC_{50} to the low nanomolar range (Table 2). Small changes in structure, such as a substituted phenyl group, led to more ion channel activity (**2a** and **2b**). The employment of an acid moiety (**2c**) removed ion channel issues but introduced a 40-fold right shift of the IC_{50} in the DHET assay vs its human sEH IC_{50}. Among three pyridine regioisomers (**2d**, **2e**, and **2f**), **2d** displayed the cleanest off-target profiles and the best enzyme activity. Of the two enantiomers of **2d**, the eutomer (*ent*A-**2d**) was 4-fold more active than the distomer (*ent*B-**2d**) against the human sEH. Not only was *ent*A-**2d** inactive in ion channel and CYP enzyme assays, it was also selective against sEH vs a panel of 166 counterscreening targets (IC_{50} > 10 μM) including a subset involved in blood pressure regulation. The X-ray crystallographic structure of *ent*A-**2d** established its absolute configuration shown in the first entry of Table 3. The pyrazine analogue **2g** had a similar overall profile as **2d**, but pyrimidine analogue **2h** was less active in inhibiting sEH and more active in inhibiting CYP2C9. Finally, bicyclic heterocycles such as isoquinoline or quinoline resulted in increased ion channel and CYP activity (**2i** and **2j**).

Table 3 summarizes the optimization of the right hand of the molecule toward the identification of the phenylcyclopropyl group as the optimized moiety, likely due to its aromatic nature and conformational rigidity. Although aniline

Table 3. In Vitro SAR on sEH and mEH Inhibition, DHET Production, CYP and Ion Channels[a]

Compds	IC_{50} (h, r) (nM)	DHET IC_{50}, (nM)[b]	mEH IC_{50} (μM)[c]	CYP2C9, 2D6, 3A4 IC_{50} (μM)	DLZ, IKr $Na_v1.5$ IC_{50} (μM)
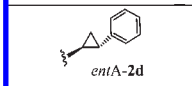	14, 27	18	>100	>10, >10, >10	>30, >30, >10
*ent*A-**2d**					
	7, 17	7	-	>10, >10, >10	15, 8, >10
3a					
	36, 15	181	>100	<10, >10, ~10	30, 25, >10
3b					
	8, 22	49	>100	<10, <10, <10	>30, 6, >10
3c					
	130, 610	1200	>100	-	-
3d					

[a] Activity was determined in triplicate with 20% deviation. [b] The conversion of 14,15-EET to 14,15-DHET was measured in HEK293 cells. [c] Human mEH was used.

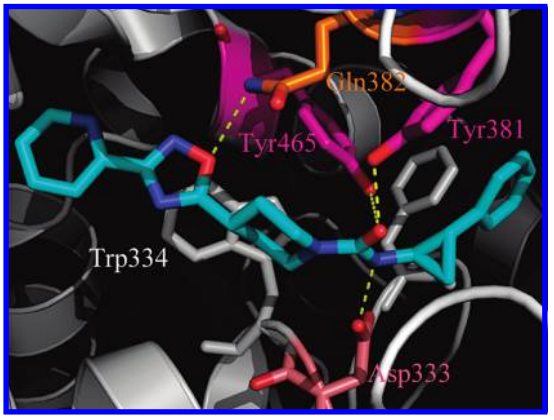

Figure 2. Minimized docking model of *ent*A-**2d** (blue) in human sEH. The dashed lines illustrate atom pairs within hydrogen bond distance. The pictures were prepared by PyMOL (Delano Scientific LLC, South San Francisco, CA). The model is based on the X-ray crystallographic structure of 1ZD3 (PDB code): human sEH 4-(3-cyclohexyluriedo)butyric acid complex.[16]

analogues such as **3a** provided better activity in sEH and DHET assays, they were associated with more ion channel issues and potentially carcinogenic metabolites. Other benzene-fused cycloalkyl groups gave worse sEH inhibition or more off-target activity.

To rationalize its good inhibitory activity, a docking model of *ent*A-**2d** in human sEH was established on the basis of the X-ray crystallographic structure of the previously reported protein−inhibitor complex (Figure 2).[16] Besides the anticipated hydrogen bond interactions between the urea N−H and Asp333 and between the urea carbonyl and Tyr381/Tyr465, an interesting hydrogen bond was identified between the oxidazole oxygen atom and Gln382. Furthermore, a $\pi-\pi$ stacking interaction of the oxidazole and the indole ring of Trp334 may further contribute to the inhibitor's good binding affinity.

An in vitro DHET production assay was employed to determine sEH inhibitory activity in SHR whole blood. Analogues **1i**, **2d**, and **2g** exhibited excellent inhibition of DHET production (91%, 92%, and 94%, respectively) 1 h

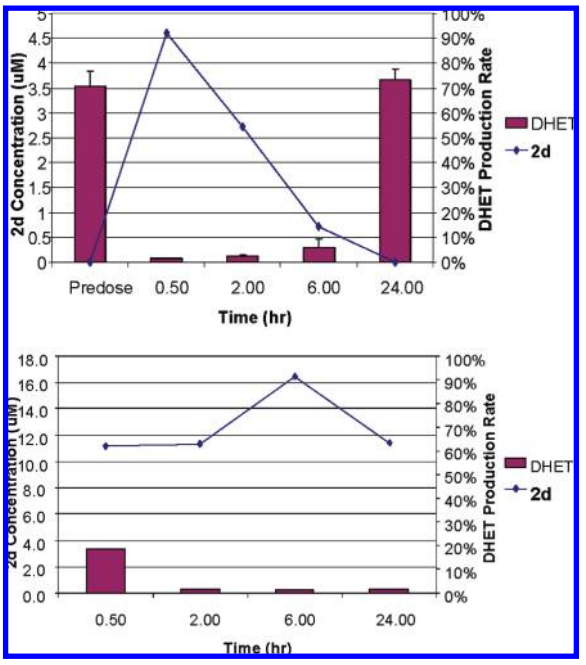

Figure 3. Ex vivo target engagement of **2d** in SHR blood (top, 50 mpk, po; bottom, 300 mpk, po). DHET production rate = (14, 15-DHET concentration (**2d**))/(14,15-DHET concentration (vehicle)).

after mixing each of the compounds (1 μM) with 14,15-EET (10 μM) in blood. Given the good PK profile of **2d** (bioavailability (77%), clearance (29 (mL/min)/kg), normalized oral exposure (1.2 μM·h·kg/mg)) and in vitro whole blood activity, the ex vivo target engagement of **2d** was evaluated after a single dose of inhibitor. At 0.5, 2, 6, 24 h postdosing, 14,15-EET was added to the blood freshly drawn, and the 14,15-DHET production rate was measured. At 50 mpk, **2d** reduced the DHET production rate to less than 10% of the control group during a time course of 0.5−6 h. In addition, an inverse correlation of the compound level and the DHET production was established (Figure 3, top). At 300 mpk, the DHET production rate in blood was diminished to less than 5% from 2 to 24 h postdose, with over 10 μM compound coverage throughout this period (Figure 3, bottom). Furthermore, **2d** demonstrated marked target engagement in SHR kidney, as evidenced by an 85% and 90% reduction in 14,15-DHET production at 50 and 300 mpk, respectively. The high dose of **2d** to achieve good target engagement reflected its serum shift, which was corroborated by rat plasma protein binding (11% free fraction in 100% rat plasma at 2.5 μM **2d**).

With excellent target engagement and specificity, the acute action of *ent*A-**2d** on vascular tone was evaluated by SHR mesenteric artery assay. Both *ent*A-**2d** and *ent*B-**2d** were able to reverse vascular contraction induced by methoxamine (IC_{50} = 6.5 and 15 μM for *ent*A-**2d** and *ent*B-**2d**, respectively), an α1-adrenergic agonist.[17] No vasoconstriction was observed on basal tension with either compound up to 100 μM. These results were in line with the vasodilatory effect of EETs previously reported in literature.[18] However, in telemetrized SHRs, *ent*A-**2d** failed to demonstrate antihypertensive activity acutely over 24 h or chronically (300 mpk, po, q.d., 7 d). A parallel PK study in SHRs confirmed excellent compound exposure on the eighth day of dosing: 35 and 20 μM at 4 and 24 h postdose, respectively. Meanwhile the endogenous epoxide/diol ratios in kidney were increased 2- to 9-fold (Figure 4,

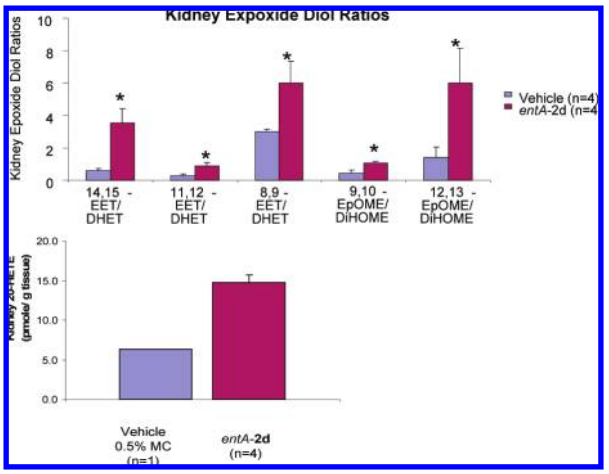

Figure 4. Effect of *ent*A-**2d** in vivo treatment (300 mpk, po, 8 d) on SHR kidney epoxide/diol ratios and 20-HETE level (EpOME = epoxide of linoleic acid, DiHOME = diol of linoleic acid).

Scheme 1[a]

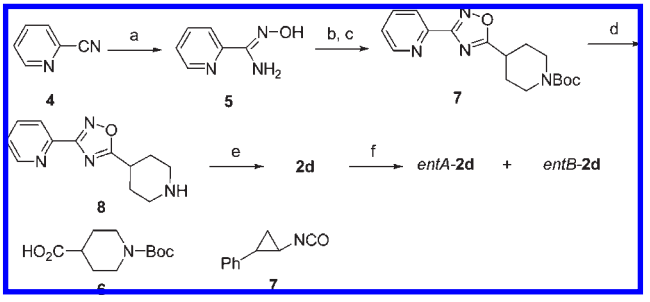

[a] Reagents: (a) $NH_2OH \cdot HCl$ salt, NaOH, EtOH, 0 °C to room temp, 94%; (b) **6**, EDCI, CH_2Cl_2, room temp, 89%; (c) cat. H_2SO_4, 120 °C, 62%; (d) TFA, CH_2Cl_2, 0 °C to room temp, 93% (e) **7**, TEA, CH_2Cl_2, room temp, 89%; (f) chiral OD (40% MeOH/CO_2, 2.1 mL/min, 100 bar, 40 °C).

top). Moreover, 20-hydroxyeicosatetraenoic acid (20-HETE), a potent vasoconstrictor,[19] was measured in SHR kidney (Figure 4, bottom). The lack of systolic blood pressure reduction by *ent*A-**2d** may be explained by invoking the 2.5-fold increase of 20-HETE, which could negate the vasodilatory effect of elevated EETs. It remains unclear whether the 20-HETE elevation resulted from the increased EETs. It is also likely that sEH inhibition by itself does not elicit a robust blood pressure effect in telemetrized SHRs.

The synthesis of racemate **2d** commenced with cyanopyridine **4** (Scheme 1). The hydroxyamine addition to cyanide **4** provided hydroxyamidine **5**, which then underwent a cyclization with acid **6** to afford oxadiazole **7**. The Boc-deprotection followed by the urea formation and a chiral SFC separation yielded two enantiomers *ent*A-**2d** and *ent*B-**2d**.

In summary, several 4-substituted piperidine-based trisubstituted ureas were discovered as highly selective and potent sEH inhibitors. In particular, **2d** inhibited sEH activity effectively in vitro, ex vivo, and in vivo. This compound also demonstrated significant vasodilatory activity in rat mesenteric artery.

Supporting Information Available: Experimental procedures for compound preparation, characterization data, and biological assay protocols. This material is available free of charge via the Internet at http://pubs.acs.org.

References

(1) (a) Newman, J. W.; Morisseau, C.; Hammock, B. D. Epoxide hydrolases: their roles and interactions with lipid metabolism. *Prog. Lipid Res.* **2005**, *44*, 1–51. (b) Hammock, B. D.; Storms, D. H.; Grant, D. F. Epoxide Hydrolases. In *Comprehensive Toxicology*; Guengerich, F. P., Ed.; Pergamon: Oxford, U.K., 1997; Vol. 3, pp 283–305.

(2) Fretland, A. J.; Omiecinski, C. J. Epoxide hydrolases: biochemistry and molecular biology. *Chem.-Biol. Interact.* **2000**, *129*, 41–59.

(3) (a) Spector, A. A.; Fang, X.; Snyder, G. D.; Weintraub, N. L. Epoxyeicosatrienoic acids (EETs): metabolism and biochemical function. *Prog. Lipid Res.* **2004**, *434*, 55–90. (b) Larsen, B. T.; Gutterman, D. D.; Hatoum, O. A. Emerging role of epoxyeicotrienoic acids in coronary vascular function. *Eur. J. Clin. Invest.* **2006**, *36*, 293–300.

(4) Larsen, B. T.; Miura, H.; Hatoum, O. A.; Campbell, W. B.; Hammock, B. D.; Zeldin, D. C.; Falck, J. R.; Gutterman, D. D. Epoxyeicosatrienoic and dihydroxyeicosatrienoic acids dilate human coronary arterioles via BK_{ca} channels: implications for soluble epoxide hydrolase inhibition. *Am. J. Physiol.: Heart Circ. Physiol.* **2006**, *290*, H491–H499.

(5) Archer, S. L.; Gragasin, F. S.; Wu, X.; Wang, S.; McMurty, S.; Kim, D. H.; Platonov, M.; Koshal, A.; Hashimoto, K.; Campbell, W. B.; Falck, J. R.; Michelakis, E. D. Endothelium-derived hyperpolarizing factor in human internal mammary artery is 11,12-epoxyeicosatrienoic acid and causes relaxation by activating smooth muscle BK (Ca) channels. *Circulation* **2003**, *107*, 769–776.

(6) Node, K.; Huo, Y.; Ruan, X.; Yang, B.; Spiecker, M.; Ley, K.; Zeldin, D. C.; Liao, J. K. Anti-inflammatory properties of cytochrome P450 epoxygenase-derived eicosanoids. *Science* **1999**, *285*, 1276–1279.

(7) Kessler, P.; Popp, R.; Busse, R.; Schini-Kerth, V. B. Proinflammatory mediators chronically downregulate the formation of the endothelium-derived hyperpolarizing factor in arteries via a nitric oxide/cyclic GMP-dependent mechanism. *Circulation* **1999**, *99*, 1878–1884.

(8) Imig, J. D.; Zhao, X.; Zaharis, C. Z.; Olearczyk, J. J.; Pollock, D. M.; Newman, J. W.; Kim, I.-H.; Watanabe, T.; Hammock, B. D. An orally active epoxide hydrolase inhibitor lowers blood pressure and provides renal protection in salt-sensitive hypertension. *Hypertension* **2005**, *46*, 975–981.

(9) Yu, Z.; Xu, F.; Huse, L. A.; Morisseau, C.; Draper, A. J.; Newman, J. W.; Parker, C.; Graham, L.; Engler, M. M.; Hammock, B. D.; Zeldin, D. C.; Droetz, D. L. Soluble epoxide hydrolase regulates hydrolysis of vasoactive epoxyeicosatrienoic acids. *Circ. Res.* **2000**, *87*, 992–998.

(10) http://www.aretetherapeutics.com.

(11) Hwang, S. H.; Tsai, H.-J.; Liu, J.-Y.; Morisseau, C.; Hammock, B. D. Orally bioavailable potent soluble epoxide hydrolase inhibitors. *J. Med. Chem.* **2007**, *50*, 3825–3840.

(12) Morisseau, C.; Newman, J. W.; Dowdy, D. L.; Goodrow, M. H.; Hammock, B. D. Inhibition of microsomal epoxide hydrolases by ureas, amides and amines. *Chem. Res. Toxicol.* **2001**, *14*, 409–415.

(13) Jamieson, C.; Moir, E. M.; Rankovic, Z.; Wishart, G. Medicinal chemistry of hERG optimizations: highlights and hang-ups. *J. Med. Chem.* **2006**, *49*, 5029–5046 and references therein .

(14) Fissthaler, B.; Hinsch, N.; Chataigneau, T.; Popp, R.; Kiss, L.; Busse, R.; Fleming, I. Nifedipine increases cytochrome P4502C expression and endothelium-derived hyperpolarizing factor-mediated responses in coronary arteries. *Hypertension* **2000**, *36*, 270–275.

(15) Viswanathan, P. C.; Balser, J. R. Inherited sodium channelopathies: a continuum of channel dysfunction. *Trends Cardiovasc. Med.* **2004**, *14*, 28–35.

(16) Gomez, G. A.; Morisseau, C.; Hammock, B. D.; Christianson, D. W. Human soluble epoxide hydrolase: structural basis of inhibition by 4-(3-cyclohexylureido)-carboxylic acids. *Protein Sci.* **2006**, *15*, 58–64.

(17) Holck, M. I.; Jones, C. H. M.; Haeusler, G. Differential interaction of clonidine and methoxamine with the postsynaptic α-adrenoceptor of rabbit main pulmonary artery. *J. Cardiovasc. Pharmacol.* **1983**, *5*, 240–248.

(18) Campbell, W. B.; Gebremedhin, D.; Pratt, P. F.; Harder, D. R. Indentification of epxoyeicosatrienoic acids as endothelium-derived hyperpolarizing factors. *Circ. Res.* **1996**, *78*, 415–423 and references therein .

(19) McGiff, J. C.; Quilley, J. 20-HETE and the kidney: resolution of old problems and new beginnings. *Am. J. Physiol.* **1999**, *277*, R607–R623.